Journal of Urban and Environmental Engineering
E-ISSN: 1982-3932
celso@ct.ufpb.br
Universidade Federal da Paraíba
Brasil

Veetil Nidheesh, Puthiya; Gandhimathi, Rajan; Thanga Ramesh, Sreekrishnaperumal; Anantha Singh, Tangappan Sarasvathy

ADSORPTION AND DESORPTION CHARACTERISTICS OF CRYSTAL VIOLET IN BOTTOM ASH COLUMN

Journal of Urban and Environmental Engineering, vol. 6, núm. 1, 2012, pp. 18-29
Universidade Federal da Paraíba
Paraíba, Brasil

Available in: http://www.redalyc.org/articulo.oa?id=283223559003

Journal of Urban and Environmental Engineering, v. 6, n. 1, p 18-29

ISSN 1982-3932
doi: 10.4090/juee.2011.v6n1.018029

Journal of Urban and Environmental Engineering

www.journal-uee.org

ADSORPTION AND DESORPTION CHARACTERISTICS OF CRYSTAL VIOLET IN BOTTOM ASH COLUMN

Puthiya Veetil Nidheesh[1], Rajan Gandhimathi[2*], Sreekrishnaperumal Thanga Ramesh[3] and Tangappan Sarasvathy Anantha Singh[1]

[1]M. Tech. Graduate, Department of Civil Engineering, National Institute of Technology, Tiruchirappalli. Tamilnadu, India;
[2]Assistant Professor, Department of Civil Engineering, National Institute of Technology, Tiruchirappalli. Tamilnadu, India.
[3]Associate Professor, Department of Civil Engineering, National Institute of Technology, Tiruchirappalli. Tamilnadu, India.

Received 16 December 2011; received in revised form 25 April 2012 accepted 06 May2012

Abstract: This study described adsorption of Crystal Violet (CV) by bottom ash in fixed-bed column mode. Equilibrium of adsorption was studied in batch mode for finding adsorption capacity of bottom ash. In fixed bed column adsorption, the effects of bed height, feed flow rate, and initial concentration were studied by assessing breakthrough curve. The slope of the breakthrough curve decreased with increasing bed height. The breakthrough time and exhaustion time were decreased with increasing influent CV concentration and flow rates. The effect of bed depth, flow rate and CV concentration on the adsorption column design parameters were analyzed. Bed depth service time (BDST) model was applied for analysis of crystal violet adsorption in the column. The adsorption capacity of bottom ash was calculated at 10% breakthrough point for different flow rates and concentrations. Desorption studies reveals that recovery of CV from bottom ash was effective by using CH_3COOH than H_2SO_4, NaOH, HCl and NaCl solutions.

Keywords: Adsorption; Crystal violet; Bottom ash; fixed bed; BDST

* Correspondence to: Rajan Gandhimathi, Tel:+91 431 2503171; Fax: +91 431 2500133
E-Mail: rgmathii@nitt.edu

INTRODUCTION

Dyes are the one of the major constituents of the wastewater produced from many industries related to textile, paint and varnishes, ink, plastics, pulp and paper, cosmetics, tannery etc., and also to the industries, which produces dyes (Adak *et al.*, 2005). Textile mill effluents are generally characterized by the parameters of BOD, COD, pH, suspended solids and color. Most of these parameters are removed satisfactorily by conventional chemical coagulation and biological treatment methods except highly polymer structured color (Selcuk, 2005).

The dyes are one important part of the pollution problem as it is estimated that 50% of their amount is not fixed on fibers and remain finally in wastewater (Harrelkas *et al*., 2009). Dyes concentration in effluents is usually lower than any other chemical found in these wastewaters, but due to their strong color they are visible even at very low concentrations, thus causing serious aesthetic problems in wastewater disposal (Zollinger, 2003). Environmental pollution by dyes also set a severe ecological problem which is increased by the fact that most of them and their degradation by-products are difficult to discolor and degrade using standard biological methods (Al-Momani *et al*., 2002). Uptake of textile effluents through food chain in aquatic organisms may cause various physiological disorders like hypertension, sporadic fever, renal damage, cramps etc. The bio-accumulation of organic and inorganic toxicants depends on availability and persistence of the contaminants in water, food and physiological properties of the toxicants (Karthikeyan *et al*., 2006).

Adsorption is widely used in the removal of refractory pollutants (including dye) from wastewater. The major advantages of an adsorption treatment for the control of water pollution are less investment in terms of initial development cost, simple design, easy operation, and free from or less generation of toxic substances (Crini, 2006).

Adsorption onto activated carbon has been found to be superior for wastewater treatment compared to other physical and chemical techniques, such as flocculation, coagulation, precipitation and ozonation as they possess inherent limitations such as high cost, formation of hazardous by-products and intensive energy requirements (Padmesh *et al.*, 2006). Even though activated carbon showed advantages, the main drawback of the activated carbon is the cost and difficulty in regeneration (Liu *et al*., 2007). Therefore, in recent years, this has prompted a growing research interest in the production of activated carbons from renewable and cheaper precursors which are mainly industrial and agricultural by-products (Tan *et al.*, 2008).

Various low-cost adsorbents from industrial by-products have been investigated to remove dyes from 2004a) and fly ash (Rachakornkij *et al.*, 2004). Bottom ash is one of such low cost adsorbent. The bottom ash is a coarse, granular, incombustible by-product of power plants, obtained after combusting coke. It is an undesired collected material, whose disposal has always been a matter of concern to the station authorities, as the dumped ash makes the land infertile (Hecht & Duvall, 1975). Already proved that bottom ash was very efficient adsorbent for removing Malachite Green (Gupta *et al*., 2004b), Quinoline Yellow (Gupta *et al*., 2005), Acid Orange 7 (Gupta *et al*., 2006a), 2-Aminophenol (Gupta *et al*., 2006b), Basic fuchsin (Gupta *et al*., 2008), Carmoisine A (Gupta *et al*., 2009), Chrysoidine Y (Mittal *et al.*, 2010a) and Crystal Violet (Mittal *et al.*, 2010b). But there are seldom publications about the dye adsorption behavior of bottom ash in column mode. Both batch adsorption and fixed-bed adsorption studies are required to obtain key parameters required for the design of fixed-bed adsorber (Song *et al*., 2011).

Keeping these in view it was considered worthwhile to use bottom ash as an adsorbent for the removal of crystal violet (CV) from aqueous solution. Crystal violet, also known as Basic Violet 3, is a well-known cationic dye being used for various purposes: a biological stain, a dermatological agent, a veterinary medicine, an additive to poultry feed to inhibit propagation of mold, intestinal parasites and fungus etc. It is also extensively used in textile dying and paper printing (Adak *et al*., 2005). Mass Transfer Zone (MTZ) and breakthrough characteristics were studied for CV adsorption in bottom ash column for different flow rate, bed depth and initial CV concentration. Bed Depth Service Time Model (BDST), which offers a simple approach and rapid prediction of adsorber performance, was applied for modeling adsorption of CV in bottom ash column.

MATERIALS AND METHODS

Adsorbent and adsorbate

The thermal power plant waste material, 'Bottom ash' (size of 300 to 600 μm) was utilized as potential adsorbent in this study. The adsorbent was obtained from Neyveli Lignite Corporation Limited, Neyveli, Tamilnadu, India. Crystal Violet (A.R Grade, C.I.42555, λ_{max} = 579 μm, Molecular weight = 407.99 g/mol, Molecular Formula = C_{25} $H_{30}Cl$ N_3), from S.D. fine chem. Pvt Ltd, was the adsorbate used for this study. The chemical structure of Crystal violet is shown in **Fig. 1**.

SEM and FTIR study

Most of the characteristics of bottom ash were given in our previous work (Nidheesh *et al.*, 2011). Scanning

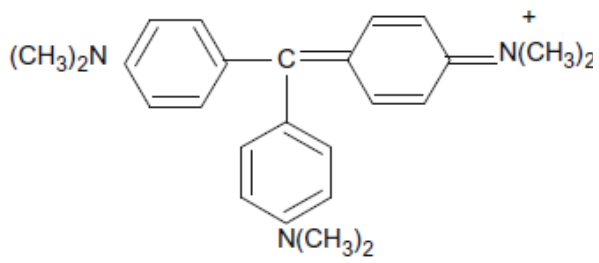

Fig. 1 Chemical structure of crystal violet.

bottom ash to study their surface textures. The SEM analysis was done at 1000× magnification. In addition, the surface functional groups of bottom ash were detected by Fourier Transform Infrared (FTIR) Spectroscope (FTIR-2000, Perkin Elmer) using KBr pellet method. The spectra were recorded from 4000 to 400 cm^{-1}. SEM and FTIR were carried out for bottom ash after adsorption to find their changes in respective characteristics.

Adsorption isotherm

The batch sorption studies were carried out by shaking a series of bottles containing different amounts of Bottom ash dosage (0.08 to 0.53) in 100 mL of 10 mg/L dye solution prepared in the laboratory. The samples were stirred at room temperature at 150 rpm for equilibrium time, and their content was then centrifuged at 3500 rpm for 5 min and the supernatant liquid was analyzed for dye concentration. An IHC- 3280 Orbital shaking incubator was used for batch adsorption experiments. A UV/Vis spectrophotometer (Lambda 25) was used for measurement of dye concentration.

Column studies

Fixed bed column studies were conducted using columns of 2 cm diameter and 50 cm length. The column was packed with bottom ash between two supporting layers of pre equilibrated glass wool and glass beads. The schematic diagram of the column study is shown in **Fig. 2**. The particle size was 300–600 µm with a bed depth of 30 cm and filling weight of 45.98 g.

The packed density or bulk density of the adsorbent in the column was approximately 0.312 g cm^{-3}. The dye solution was fed through the fixed-bed column in the down flow mode. Before operation, the bed was rinsed with distilled water and left overnight to ensure a closely packed arrangement of particles with no void, channels, or cracks. The effluent samples were collected at specified time intervals and measured for the dye concentration by UV/Vis spectrophotometer. The flow to the column was continued until the effluent concentration (C) approached the influent concentration (C_0).

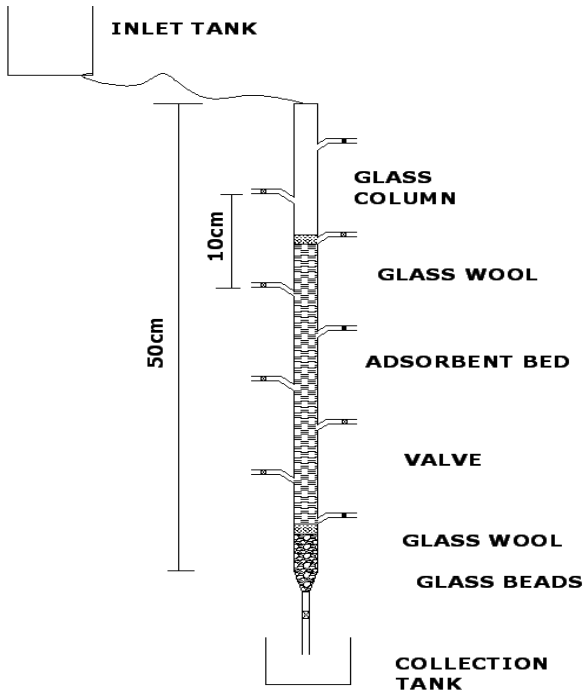

Fig. 2 Schematic diagram of lab-scale column study.

The effects of the following parameters, on crystal violet adsorption were investigated. (a) Effect of bed height: bed height was varied between 10 to 30 cm, keeping flow rate and initial CV concentration constant (b) Effect of flow rate: flow rate was varied between 10 and 20 mL/min, while bed height and initial CV concentration were held constant (c) Effect of initial CV concentration: initial CV concentration was varied among 10, 15 and 25 mg/L at constant bed height and flow rate.

Design parameters of adsorption column

When adsorbate is introduced at the top of a clean bed of adsorbent, most solute removal initially occurs at top of column in a rather narrow band at the top of column, known as adsorption zone (Benfield *et al.*, 1982). When the adsorption zone moves down and the lower edge of this zone reaches the bottom of the column, the effluent concentration starts to rise rapidly (Faust & Aly, 1987).

The point at which the effluent concentration increases rapidly is known as breakthrough point. When the effluent concentration C is approaching to 90% of C_0 (initial adsorbate concentration) then the adsorbent is considered to be essentially exhausted. As per Benfield *et al*. (1982) depth of exchange zone, time required for exchange zone to move its own height, adsorption rate, adsorption capacity etc. are the main design parameters of adsorption column.

The time required for the exchange zone to move the length of its own height up/down the column once it has become established is:

$$t_z = \frac{(V_E - V_B)}{r} \quad (1)$$

where V_E = total volume of wastewater treated to the point of exhaustion (L); V_B = total volume of wastewater treated to the point of breakthrough (L); r = wastewater flow rate (L/hr).

The time required for the exchange zone to become established and move completely out of the bed is:

$$t_E = \frac{V_E}{r} \quad (2)$$

Rate at which the exchange zone is moving up or down through the bed is:

$$U_z = \frac{h_z}{t_z} = \frac{h}{t_E - t_f} \quad (3)$$

where, h_z = height of exchange zone (cm); h = total bed depth (cm); t_f = time required for the exchange zone to initially form (h). Rearranging **Eq. (3)** provides an expression for the height of the exchange zone as given below.

$$h_z = \frac{ht_z}{t_E - tf} \quad (4)$$

The value of t_f can be calculated as follows:

$$t_f = (1 - F)t_z \quad (5)$$

At breakthrough, the fraction (F) of adsorbent present in the adsorption zone still possessing ability to remove solute is:

$$F = \frac{S_z}{S_{\max}} = \frac{\int_{V_B}^{V_E} (C_o - C)\,dV}{C_o (V_E - V_B)} \quad (6)$$

where, C_o = initial solute concentration (mg/L); S_z = amount of solute that has been removed by the adsorption zone from breakthrough to exhaustion; $S_{\max}$ = amount of solute removed by the adsorption zone if completely exhausted. The percentage of the total column saturated at breakthrough is

$$\%saturation = \frac{h + (F - 1)h_z}{h} \times 100 \quad (7)$$

Weber (1972) gives an equation for height of MTZ as a function of volume as:

$$h_z = h\left(\frac{V - V_B}{V_E - V_B}\right) \quad (8)$$

Desorption study

Desorption studies help to elucidate the nature of adsorption and recycling of the spent adsorbent and the dye. If the adsorbed dyes can be desorbed through using neutral pH water, then the attachment of the dye of the adsorbent is by weak bonds (Ansari & Mosayebzadeh, 2010). Desorption study was carried out in batch followed by column methods. For batch study, 1N solution of H_2SO_4, NaOH, CH_3COOH, HCl, and NaCl (50mL each) is used for saturated adsorbent and kept in shaker up to 1 h. The sorbent solution mixtures were then centrifuged at 3600 rpm for 5 minutes and the supernatant was analyzed for the dye concentration.

The chemical reagent having higher CV recovery in batch mode was used for column study. Column saturated with 20 mL/min with CV of 25 mg/L has been selected for desorption study. The reagent was passed through the column at a flow rate of 15 mL/min slightly less than 20 mL/min. Effluent concentration was noted in an interval, in order to analyze desorption behavior of CV in bottom ash column.

RESULTS AND DISCUSSION

Adsorption isotherms

The adsorption isotherm indicates how the adsorption molecules distribute between the liquid phase and the solid phase when the adsorption process reaches an equilibrium state (Bello *et al.*, 2010). The simplest proposed model for characterizing adsorption is the Langmuir isotherm. The Langmuir isotherm is developed by assuming that a fixed number of adsorption sites are available, and that the adsorption is reversible. The Langmuir isotherm may be used when the adsorbent surface is homogeneous. The Langmuir isotherm is expressed as (Langmuir, 1915).

$$q_e = \frac{X}{M} = \frac{q_{\max}\, b\, C}{1 + b\, C} \quad (9)$$

where b is constant that increases with increasing molecular size, $q_{\max}$ is amount adsorbed to form a complete monolayer on the surface (mg/g), X is weight of substance adsorbed (mg), M is weight of adsorbent (g), and C is concentration remaining in solution (mg/L). The above equation can be recast in a linear form as:

$$\frac{1}{X/M} = \frac{1}{q_{\max}} + \frac{1}{q_{\max} b}\frac{1}{C} \quad (10)$$

Isotherm plot for the removal of CV onto bottom ash

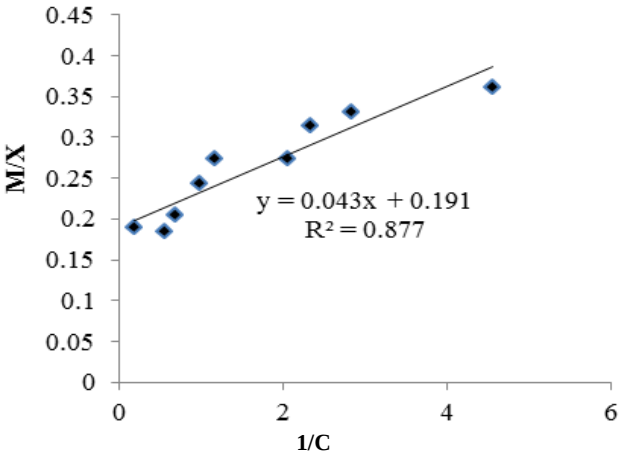

Fig. 3 Langmuir isotherm for CV removal by bottom ash.

From **Fig. 3**, regression values (R^2) indicates that the adsorption data for CV onto bottom ash fitted well with the Langmuir isotherm. The intercept and slope of straight line were used to obtain the Langmuir constants. Langmuir constants b and q_{max} were evaluated and have the value of 4.44 and 5.24 mg/g, respectively. The correlation coefficient (R^2) was obtained as 0.877.

Effect of bed-depth

Fixed-bed column studies were conducted using column packed with bottom ash for three different heights such as 10, 20 and 30 cm. The column was fed with Crystal violet solution in the down flow mode with a flow rate of 15 mL/min and the initial dye concentration of 25 mg/L. The breakthrough curves (at different masses or bed-depths) are shown in **Fig. 4**. From the **Fig. 4**, it was observed that the breakthrough and exhaustion time increases with bed depth.

The higher bed column resulted in a decrease in the effluent concentration at the same service time. The slope of the breakthrough curve decreased with increasing bed height, which resulted in a broadened mass transfer zone (Han *et al.*, 2009).

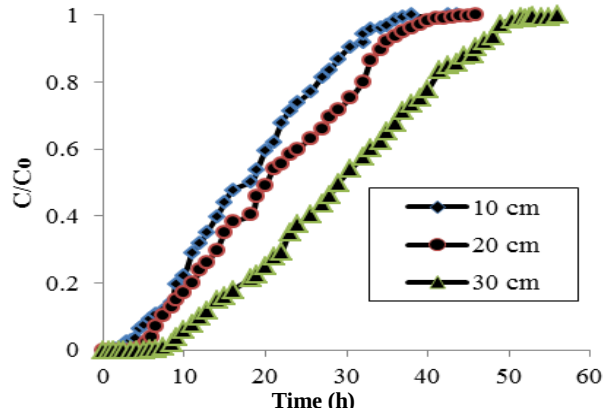

A higher CV uptake was also observed at a higher bed height due to the increase in the specific surface of the adsorbent which provided more fixation binding sites for the dye to adsorb. The increase in the adsorbent mass in a higher bed provided a greater service area which would lead to an increase in the volume of the solution treated (Tan *et al.*, 2008).

Effect of initial dye concentration

To evaluate the effect of the influent CV concentration on its reduction in the column, the concentration of CV was increased from 10 to 25 mg/L under the same operating condition. **Fig. 5** depicts three breakthrough curves of CV removal by bottom ash at different initial dye concentration, for the 10 cm bed-depth, and flow rate of 20 mL/min. It is illustrated that the breakthrough time decreased with increasing influent CV concentration. At lower influent CV concentration, breakthrough curve was dispersed and breakthrough occurred slowly. As influent concentration increased, sharper breakthrough curves were obtained. These results demonstrate that the change of concentration gradient affects the saturation rate and breakthrough time. This can be explained by the fact that more adsorption sites were being covered as the CV concentration increases (Han *et al.*, 2009).

Effect of flow rate

Columns were run at different flow rates such as 10, 15 and 20 mL/min with a fixed adsorbent bed of 10 cm at an initial CV concentration of 25 mg/L to study the effect of flow rate in the performance of bottom ash bed. The breakthrough curves at various flow rates are shown in **Fig. 6**. From the **Fig. 6**, it can be seen that the breakthrough generally occurs faster with a higher flow rate. Breakthrough times ($C/C_0 = 0.1$) were found to be 11, 6 and 3.5 h for the flow rate of 10, 15 and 20 mL/min, respectively. Similarly the exhaustion times were increased with decrease in flow rate. This is due to the fact that at a low rate of influent; CV had more time to be in contact with adsorbent, which resulted in a greater removal of CV molecules in column (Han *et al.*, 2009). At a higher flow rate, the adsorption capacity was lower due to insufficient residence time of the solute in the column and diffusion of the solute into the pores of the adsorbent, and therefore, the solute left the column before equilibrium occurred (Tan *et al.*, 2008).

Effect of bed depth, flow rate and initial CV concentration on MTZ Development

Development of MTZ with time for different depth, initial CV concentration and flow rate is shown in **Fig. 7**. Figure revealed that the mass transfer rate increases

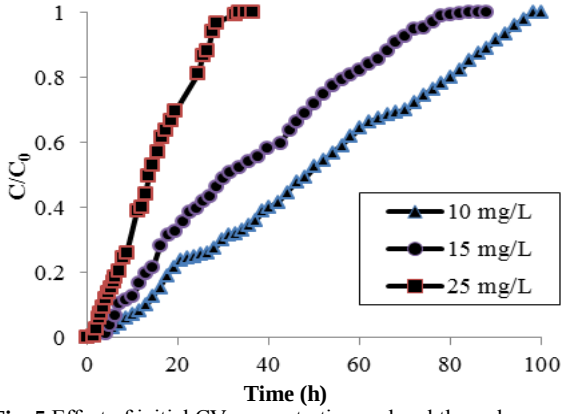

Fig. 5 Effect of initial CV concentration on breakthrough curves.

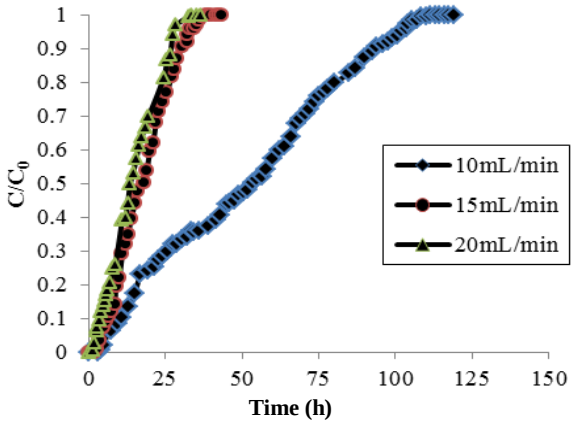

Fig. 6 Effect of flow rate on breakthrough curves.

with bed depth, initial CV concentration and flow rate. Column design parameters for different depths, initial CV concentration and flow rate are given in **Table 1**. From **Table 1**, it was found that all the design parameters excluding percentage of bed saturation increases with bed depth. Then, it was clear that the adsorption capacity of bottom ash decreases with increase in bed depth. It was also found that t_E and t_z decreases with increase in CV concentration and flow rate. But h_z and U_z increases with increase in CV concentration and flow rate.

Analysis of CV adsorption in column by BDST model

BDST is a simple model for predicting the relationship between bed depth, and service time, t, in terms of process concentrations and adsorption parameters (Han *et al*., 2009). This model is used only for the description of the initial part of the breakthrough curve, i.e. up to the breakpoint or 10–50% of the saturation points (Chen *et al.*, 2006). The objective of fixed-bed operations is to reduce the concentration in the effluent so that it does not exceed a specific breakthrough concentration (Faki *et al.*, 2008).

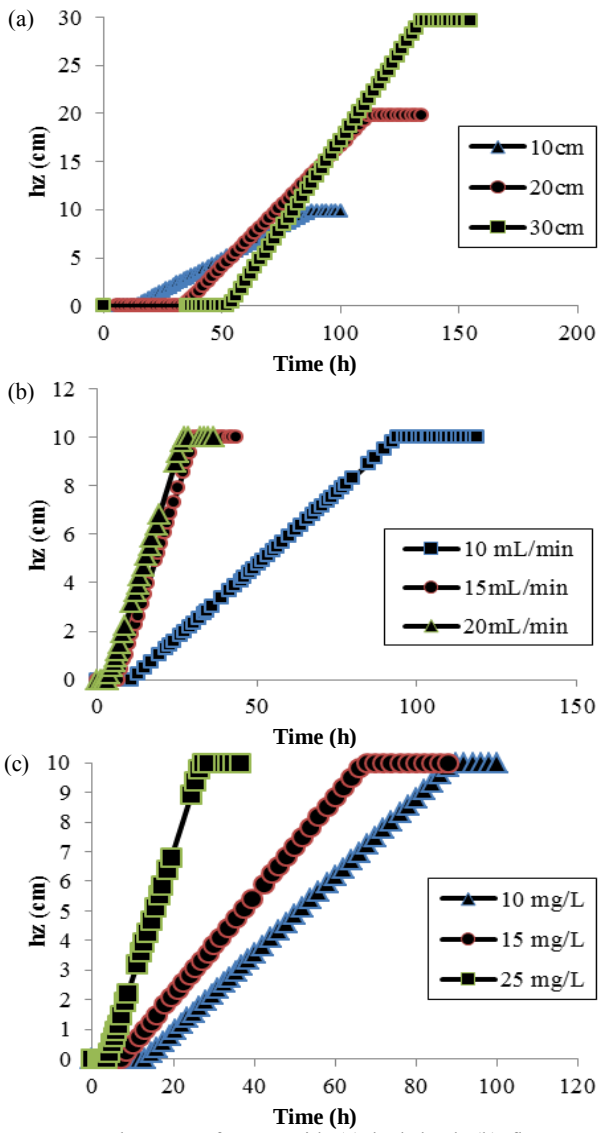

Fig. 7 Development of MTZ with (a) bed depth (b) flow rate (c) initial CV concentration.

This BDST model was focused on the estimation of characteristic parameters such as the maximum adsorption capacity and kinetic constant (Suksabye *et al*., 2008). The BDST model is based on the assumption that the rate of adsorption is controlled by the surface reaction between adsorbate and the unused capacity of the adsorbent (Goel *et al*., 2005). The original BDST theory was developed for the removal of chlorine gas by charcoal column. Adams–Bohart model (Bohart & Adams, 1920) is presented as:

$$\ln\left(\frac{C_o}{C_b}-1\right)=\ln\left(e^{K_aHN_{\%}}-1\right)-K_aC_ot \qquad (11)$$

where C_o is the initial concentration of solute (mg/L), C_B the desired concentration of solute at breakthrough

Table 1 Column design parameters

Concentration mg/L	Flow (mL/min)	Bed depth (cm)	t_E (hr)	t_z (h)	h_z (cm)	U_z (cm/h)	Bed Saturation (%)
		10	89	76	9.337	0.123	90.82
10	20	20	113	80	15.238	0.19	91.56
		30	136	83	19.5	0.235	92.13
		10	67	60	9.836	0.164	89.688
15	20	20	92	73	17.273	0.237	90.08
		30	106	80	24.49	0.306	93.351
		10	27	23.5	9.53	0.41	90.47
	20	20	34	28.5	18.33	0.64	90.8
		30	39	29	24.10	0.83	91.97
		10	30.5	24	8.54	0.36	91.46
25	15	20	34.5	29.5	18.70	0.63	90.65
		30	46	33.5	23.56	0.70	92.15
		10	94	67	7.67	0.114	91.36
	10	20	115	75	13.95	0.186	92.8
		30	126	83	21.16	0.255	93.47

(mg/L), k_a the adsorption rate constant (L/mg/h), N_o the adsorption capacity (mg/L), H the bed depth of column (cm), u the linear flow velocity of feed to bed (cm/hr), t is the service time of column under above conditions (hrs). Since $e^{K_a H N_o / u}$ always greater than 1, **Eq. (11)** reduced to:

$$t = \frac{HN_o}{uC_o} - \frac{\ln\left(C_o / C_B - 1\right)}{k_a C_o} \tag{12}$$

This is in the form of

$$t = aH - b \tag{13}$$

That is, a plot of service time t against H should generate a straight line with slope a equal to $(N_o/C_o u)$ and intercept b of $(-(1/k_a C_o)\ln((C_o/C_B)-1))$. From the slope and intercept, both N_o and k_a are calculated.

The critical bed depth (H_o) is the theoretical depth of adsorbent sufficient to ensure that the outlet solute concentration does not exceed the breakthrough concentration (C_B) value at time t = 0. H_o can be calculated as (Sarin *et al*., 2006).

$$H_o = \frac{u}{N_o k_a} \ln\left(\frac{C_o}{C_B} - 1\right) \tag{14}$$

Figure 8a shows the applied BDST curve for different concentration at a flow rate of 20 mL/min. Figure reveals that the BDST model fit very well for the experiment data. The parameters of fixed-bed column system for various flow rates and concentration are given in **Table 2**.

Adsorption capacity of bottom ash is calculated by dividing N_o by mass of adsorbent. As per model predicted values, the adsorption capacity of bottom ash increases with decrease in flow rate. But exception is there in case of 15 mL/min. This may be due to experimental error. The adsorption capacity is also increases with decrease in concentration, for a constant flow rate. The adsorption rate constant is directly proportional to flow rate. That is adsorption rate constant is decreases with decrease in flow rate and concentration. The critical bed depth is decreases with decrease in flow rate and concentration.

At 50% of breakthrough, the logarithmic term in **Eq. (12)** reduces to zero, and the final term in the BDST equation become zero, giving the relationship as (Suksabye *et al*., 2008).

$$t_{50} = \frac{N_o H}{C_o u} \tag{15}$$

If the curve of t_{50} versus H is a straight line passing through the origin, it can be explained that the adsorption data follow the BDST model (Netpradith *et al*., 2004; Zulfadhly *et al*., 2001). **Figure 8b** shows that the applied BDST curve for different experiment values at 50% breakthrough. But it is not passing through origin, even R^2 values is very high.

Table 2 Experimental constants of BDST model

Concentration (mg/L)	Flow Rate (mL/min)	u (cm/h)	N_0 (mg/cm^3)	k_a (L/ mg/h)	R^2	H_0 (cm)	q (mg/g)
10	20	381.97	7.83	0.031	0.998	3.46	170.29
15	20	381.97	5.73	0.062	0.987	2.36	124.62
	10	190.98	11.22	8.37×10^{-3}	0.978	4.47	244.02
25	15	286.47	2.32	0.035	0.982	7.75	50.46

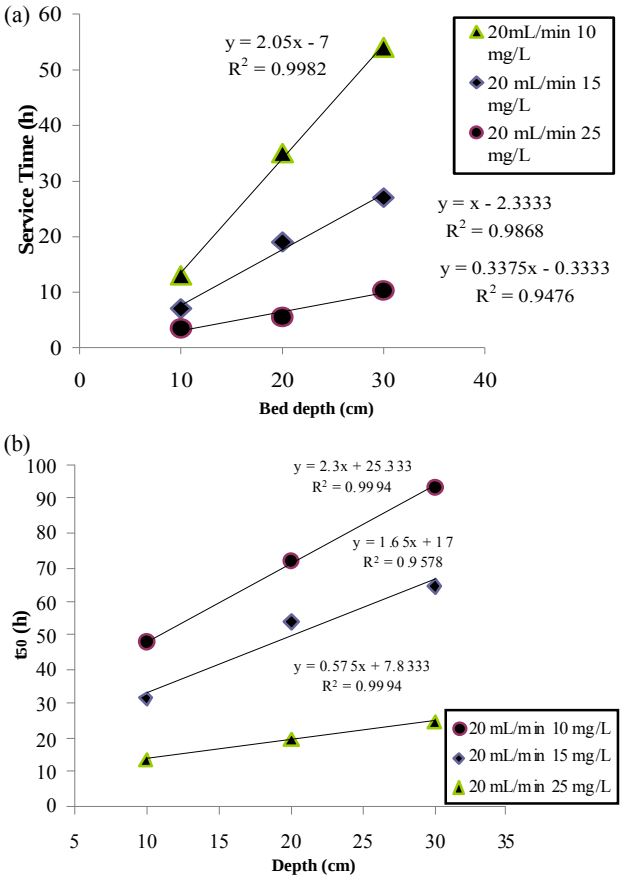

Fig. 8 BDST model for CV adsorption by Bottom ash at (a) 10% breakthrough, (b) 50% breakthrough.

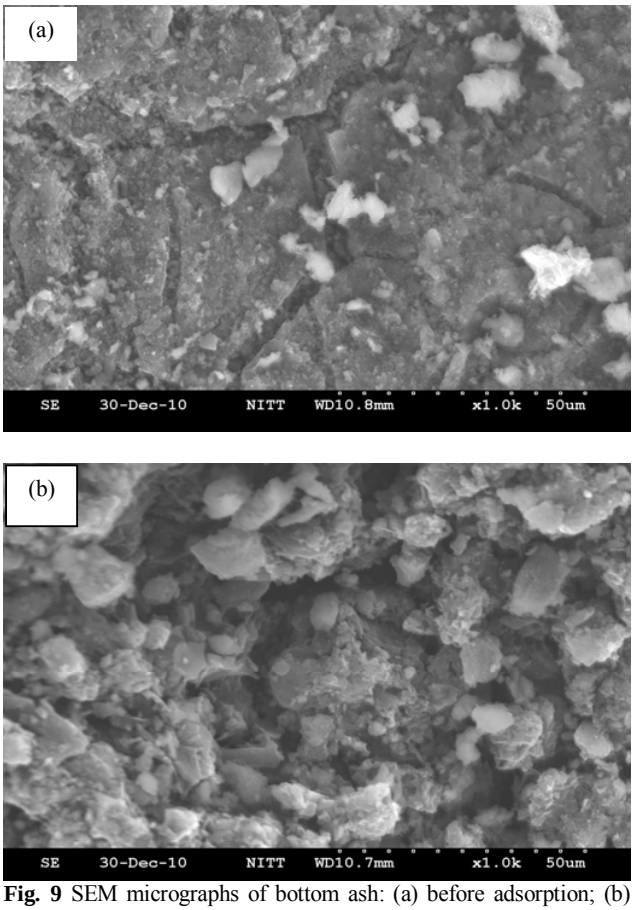

Fig. 9 SEM micrographs of bottom ash: (a) before adsorption; (b) after adsorption.

This indicates that the transport of crystal violet from the aqueous solution onto bottom ash is quite complex and involves more than one rate-limiting step (Sharma & Foster, 1995; Zulfadhly *et al*., 2001).

SEM and FTIR pattern

In order to confirm CV adsorption in bottom ash column, SEM analysis was carried out for raw and CV adsorbed bottom ash. The SEM photographs of adsorbents before and after adsorption are shown in **Figs 9a** and **9b**, respectively. From these pictures, it is clear that there was significant difference in the appearance of the adsorbent surfaces. The white clumps on the adsorbent surface represent the adsorbate (Ghosh & Liji Philip, 2005).

FTIR technique is an interesting application for studying the interaction between an adsorbate and the active groups on the surface of adsorbent (Monash & Pugazhenthi, 2009). FTIR spectroscopy was, therefore, carried out to identify the major functional groups presented in bottom ash. The FTIR spectrum of bottom ash, before and after CV adsorption, is shown in **Fig. 10**. From **Fig. 10**, it was found that bottom ash (before adsorption) have peaks at 786, 953, 1098, 1649, 3446

The peak at 2926 cm^{-1} is an indicator of the stretching vibration of the C–H group. The absorption bands at 1649, 1505 and 1407 cm^{-1} indicates the presence of COO, N–H and C–O groups on the biosorbent surface (Kumar & Ahmad, 2011). Other functional groups corresponding to each peaks is given in our previous work (Nidheesh *et al.*, 2011). In the case of bottom ash after adsorption, the percentage transmittance of peaks corresponding to 3446 cm^{-1} is increased in the bottom ash after adsorption. But the peaks at 929, 1128, 1638 and 1796 cm^{-1} are decreased in the bottom ash after adsorption.

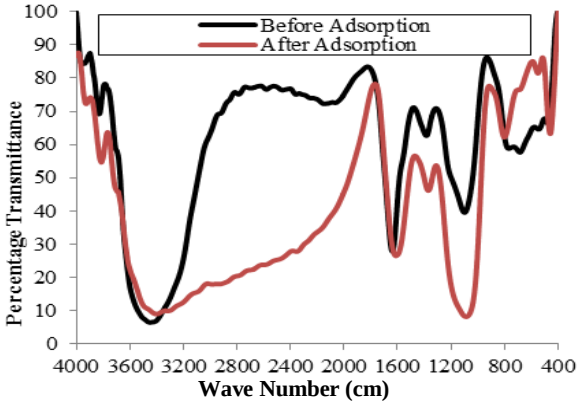

Fig. 10 FTIR Spectrum of bottom ash before and after CV

Adsorption mechanism

There were many factors that may influence the adsorption behavior, such as dye structure and size, adsorbent surface properties, stearic effect and hydrogen bonding, Vander Waals forces etc. CV is a cationic dye having amine groups in its structure. In an aqueous solution, it dissociates as (Kumar & Ahmad, 2011):

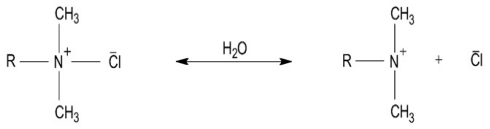

(16)

where R is used for rest of the dye molecule.

The complexation between CV and bottom ash can take place through the weak and strong forces. The weak interactions occur due to the Vander Waals forces while the strong interactions occur due to (i) hydrogen bonding interaction between the nitrogen containing amine groups of CV and bottom surface (ii) hydrophobic–hydrophobic interactions between the hydrophobic parts of CV and bottom ash (iii) electrostatic interaction between the cationic dye (due to the presence of +N $(CH_3)_2$ group) and negatively charged bottom ash surface in basic medium (Kumar & Ahmad, 2011).

On the surface of the bottom ash the functional oxidized groups are present as SiO_2 and Al_2O_3. The central ion of silicates (Si^{4+}) has a very strong affinity for electrons; therefore, the oxygen atoms that are bound to the silicon ions have a low basicity, making the silica surface act as a weak acid. The oxygen atoms on the silica surface are free to react with water, forming surface silanol (SiOH) groups. The acidity of the silanol (SiOH) groups determines the dependence of the charge of the silica surface on pH. At low pH, a positively charged silica surface results, and at high pH values negatively charged surface prevails (Mohan & Gandhimathi, 2009).

In this study, the adsorption experiments were carried out in the alkaline pH (around 8.07 at 27.7°C). From the point of zero charge of the bottom ash (pH_{PZC} = 6.2) (Nidheesh *et al.*, 2011), it was found that the silica, alumina and iron content of the bottom ash were negatively charged above 6.2 pH value. The negative charge at an active site on the surface of the bottom ash (**Eqs. 17** and **18)** which allows N^+- R (CV in aqueous solution) to be complexed at the surface (**Eqs 19** and **20**).

$$\equiv SiOH + OH^- \rightarrow \equiv SiO^- + H_2O \quad (17)$$

$$\equiv AlOH + OH^- \rightarrow \equiv AlO^- + H_2O \quad (18)$$

$$(\equiv SiO^-) + N^+\text{- R} \rightarrow (\equiv Si\text{–}O)\ N\text{- R} \quad (19)$$

$$(\equiv AlO^-) + N^+\text{- R} \rightarrow (\equiv Al\text{–}O)\ N\text{- R} \quad (20)$$

The overall mechanism of removal of CV by bottom ash is shown as in **Fig. 11**. The dotted line represents the bonding between bottom ash and CV.

Desorption study

Desorption study was done both in batch and continuous mode. Column desorption study was carried out followed by batch study. The regeneration was examined (in batch mode) using 50 mL of the selected Solvents. The results are summarized in **Table 3**. As the data show in **Table 3**, maximum desorption percentage using different desorbing solutions was found to be about 47% by CH_3COOH. Based on the batch desorption study results, CH_3COOH was used to recover CV from the saturated column packed with bottom ash.

The column with a bed depth of 30 cm and flow rate 20 mL/min saturated with 25 mg/L of CV was selected for desorption study. Desorption was carried out by 1N CH_3COOH solution through the exhausted bottom ash bed in the downward direction at a flow rate of 15 mL/min, slightly less that the sorption flow rate 20 mL/min.

The concentration of CV was measured at different time interval as shown in **Fig. 12**. It was observed that desorption cycle took 780 min, after which further desorption was negligible. The maximum concentration of CV (338.6 mg/L) was obtained at a contact time of 20 min, which is 13.54 times higher than influent CV concentration. The eluting solution was low in volume and high in concentration, which could help in easy handling and recovery and reuse of CV.

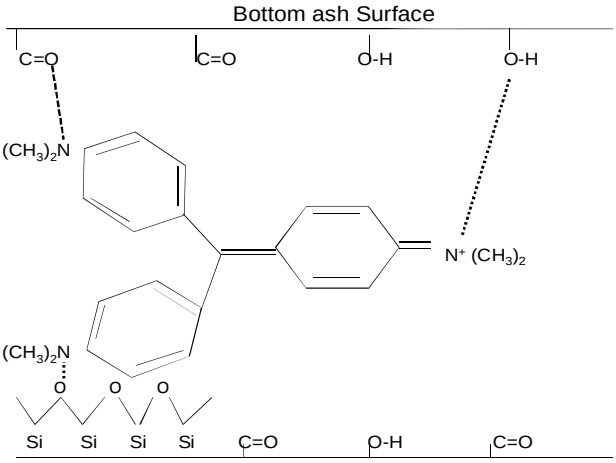

Fig. 11 Adsorption mechanism of CV removal by bottom ash.

Table 3 Desorption study for regeneration of bottom ash

Solution	Dye recovery (%)
H_2SO_4	4
NaOH	15
CH_3COOH	47
HCl	8

Recycling of regenerated column

To check the adsorption efficiency of the regenerated bottom ash column, it was reloaded with the dye solution of 25 mg/L at a rate of 20 mL/min. The breakthrough curve obtained was compared with that of raw bottom ash (10 cm depth; 25 mg/L CV concentration; flow rate of 20 mL/min) and is shown in **Fig. 13**. For raw bottom ash the breakthrough time was 4 h and exhaustion time was 27 h. But it was decreased for regenerated bottom ash. For regenerated bottom ash, breakthrough time was 2.5 h and exhaustion time was 18 h. The calculated data may prove helpful in designing a bottom ash fixed-bed for the treatment of CV of known concentration.

Desorption mechanism

CH_3COOH found to be more efficient to recover the CV from bottom ash as compared to other reagents. Addition of CH_3COOH will reduce the pH of solution. When the pH reaches less than 6.2, the surface of bottom ash predominate with positive charges. Then the bond between CV and bottom ash will break. But the regeneration capacity of CH_3COOH is very less as compared with recover of CV from *Ricinus communis* Pericarp carbon (Madhavakrishnan *et al*., 2009). Madhavakrishnan *et al*. (2009) reported that the percent desorption increased with increasing CH_3COOH concentration in the aqueous medium and attained a maximum desorption of 90% at 0.8 N CH_3COOH solution. Inefficient desorption in acetic acid indicates that CV was strongly attached onto bottom ash through chemisorptions. Similar results were observed for the adsorption of CV by treated ginger waste (Kumar & Ahmad, 2011). But addition of H_2SO_4 and HCl is ineffective to recover CV. This may be due to reaction of H_2SO_4 and HCl with CV and formation of colorless complex compounds. Similarly NaOH reacts with CV produce a colorless complex. Miertschin (2007) reported that CV reacts with NaOH and the reaction mixture color becomes less and less intense, ultimately becoming colorless when all of the crystal violet has been consumed.

CONCLUSIONS

CV adsorption onto bottom ash was investigated. Adsorption capacity of bottom ash was found to be 5.24 mg/g from batch isotherm study. Removal efficiency of dyes from wastewater strongly depends on flow rate, initial CV concentration and bed depth. The slope of the breakthrough curve decreased with increasing bed height. The breakthrough time and exhaustion time were decreased with increasing influent CV concentration and flow rates. Different column

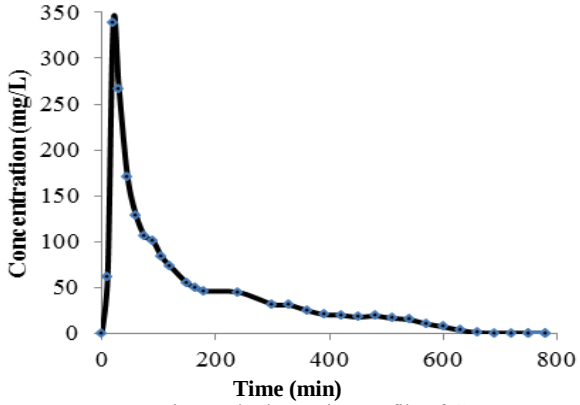

Fig. 12 First cycle desorption profile of CV.

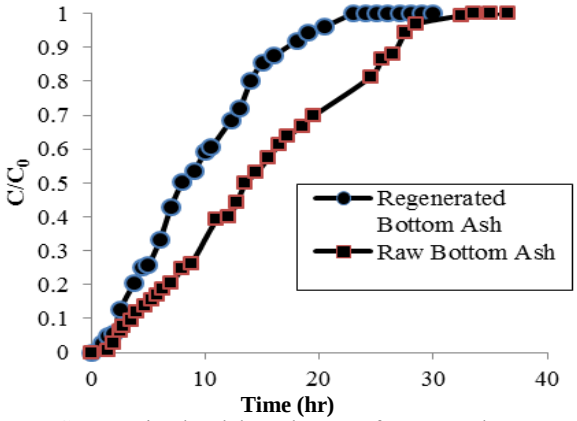

Fig. 13 Comparative breakthrough curve for raw and regenerated bottom ash.

design parameters were analyzed with respect to above three parameters. Experimental data fit well for BSDT model. BDST results show that the adsorption capacity of bottom ash inversely proportional to flow rate and concentration. Desorption studies reveals that recovery of CV from bottom ash was effective by using CH_3COOH solution.

REFERENCES

Adak, A., Bandyopadhyay, M. & Pal, A. (2005) Removal of crystal violet dye from wastewater by surfactant-modified alumina. *Sep. Purif. Technol*. **44**(2), 139–144. doi: 10.1016/j.seppur.2005.01.002

Al-Momani, F., Touraud, F., Degorce-Dumas, J.R., Roussy, J. & Thomas, O. (2002) Biodegradability enhancement of textile dyes and textile wastewater by VUV photolysis. *J. Photochem. Photobiol*. A. **153**(3), 191–197. doi: 10.1016/S1010-6030(02)00298-8

Ansari, R. & Mosayebzadeh, Z. (2010) Removal of Basic Dye Methylene Blue from Aqueous Solutions Using Sawdust and Sawdust Coated with Polypyrrole. *J. Iran. Chem. Soc*. **7**(2), 339–350.

Bello, O.S., Adelaide, O.M., Hammed, M.A. & Popoola, O.A.M. (2010) Kinetic and Equilibrium Studies of Methylene Blue Removal from Aqueous Solution by Adsorption on Treated Sawdust. *Macedonian J. Chemist. Chem. Eng.* **29**(1), 77–85.

Benfield, L.D., Weand, B.L. & Judkins, J.F. (1982) *Process chemistry for water and wastewater*. Prentice Hall Inc, Englewood Cliffs, New Jersey.

Bohart, G.S. & Adams, E.Q. (1920) Some aspects of the behavior of charcoal with respect to chlorine. *J Amer Chem Soc* **42**(6), 523–44.

Chen, G.Q., Zeng, G.M., Tu, X., Niu, C.G., Huang, G.H. & Jiang, W. (2006) Application of a byproduct of Lentinus edodes to the bioremediation of chromate contaminated water. *J. Hazardous Mater.* **135**(3), 249–255. doi: 10.1016/j.jhazmat.2005.11.060

Crini, G. (2006) Non-conventional low-cost adsorbents for dye removal: a review. *Bioresour. Technol.* **97**(9), 1061–1085. doi: 10.1016/j.biortech.2005.05.001

Faki, A., Turan, M., Ozdemir, O. & Turan, A.Z. (2008) Analysis of Fixed-Bed Column Adsorption of Reactive Yellow 176 onto Surfactant-Modified Zeolite. *Ind Eng. Chem. Res.* **47**, 6999–7004.

Faust, S.D. & Aly, O.M. (1987) *Adsorption Processes for Water Treatment*. Butterworth Publishers, Boston, Massachusetts.

Ghosh, P.K. & Liji Philip, (2005) Performance Evaluation of Waste Activated Carbon on Atrazine Removal from Contaminated Water. *J. Environm. Sci. Health Part B* **40**(3), 425–441. doi: 10.1081/PFC-200047576

Goel, J., Kadirvelu, K., Rajagopal, C. & Garg, V.K. (2005) Removal of lead (II) by adsorption using treated granular activated carbon, Batch and column studies. *J. Hazardous Mater.* **125**(3), 211–220. doi: 10.1016/j.jhazmat.2005.05.032

Gupta, V.K., Mittal, A. & Gajbe, V. (2005) Adsorption and desorption studies of a water soluble dye, Quinoline Yellow, using waste materials. *J. Colloid Interface Sci.* **284**(1), 89–98. doi: 10.1016/j.jcis.2004.09.055

Gupta, V.K., Mittal, A., Gajbe, V. & Mittal, J. (2006a) Removal and Recovery of the Hazardous Azo Dye Acid Orange 7 through Adsorption over Waste Materials, Bottom ash and De-Oiled Soya. *Ind. Eng. Chem. Res.* **45**(4), 1446-1453. doi: 10.1021/ie051111f

Gupta, V.K., Mittal, A., Gajbe, V. & Mittal, J. (2008) Adsorption of basic fuchsin using waste materials–bottom ash and deoiled soya–as adsorbents. *J. Colloid Interface Sci.* **319**(1), 30–39. doi: 10.1016/j.jcis.2007.09.091

Gupta, V.K., Mittal, A., Krishnan, L. & Gajbe, V. (2004b) Adsorption kinetics and column operations for the removal and recovery of malachite green from wastewater using bottom ash. *Separation Purification Technol.* **40**(1), 87–96. doi: 10.1016/j.seppur.2004.01.008

Gupta, V.K., Mittal, A., Malviya, A. & Mittal, J. (2009) Adsorption of Carmoisine A from Wastewater Using Waste Materials–Bottom ash and Deoiled Soya. *J. Colloid Interface Sci.* **335**(1), 24–33. doi: 10.1016/j.jcis.2009.03.056

Gupta, V.K., Suhas, Ali, I. & Saini, V.K. (2004a) Removal of Rhodamine B, Fast Green, and Methylene Blue from Wastewater Using Red Mud, an Aluminum Industry Waste. *Ind. Eng. Chem. Res.* **43**, 1740–1747.

Gupta, V.K., Mohan, D., Suhas & Singh, K.P. (2006b) Removal of 2-Aminophenol Using Novel Adsorbents. *Ind. Eng. Chem. Res.* **45**(3), 1113−1122. doi: 10.1021/ie051075k

Han, R., Wang, Y., Zhao, X., Wang, Y., Xie, F., Cheng, J. & Tang, M. (2009) Adsorption of methylene blue by phoenix tree leaf powder in a fixed-bed column, experiments and prediction of breakthrough curves. *Desalination* **245**(3), 284–297. doi: 10.1016/j.desal.2008.07.013

Harrelkas, F., Azizi, A., Yaacoubi, A., Benhammou, A. & Pons, M.N. (2009) Treatment of textile dye effluents using coagulation flocculation coupled with membrane processes or adsorption on powdered activated carbon. *Desalination* **235**(4), 330–339. doi: 10.1016/j.desal.2008.02.012

Hecht, N.L. & Duvall, D.S. (1975) *Characterization and Utilization of Municipal and Utility Sludges and Ashes*, vol III, Utility Coal Ash National Environmental Research Center, US Environmental Protection Agency.

Karthikeyan, S., Jambulingam, M., Sivakuma, P., Shekhar, A.P. & Fish Mastacembelus Armatus (Cuv & Val). *E-Journal of Chemistry* **3**(13), 303–306.

Kumar, R. & Ahmad, R. (2011) Biosorption of Hazardous Crystal Violet Dye from Aqueous Solution onto Treated Ginger Waste (TGW). *Desalination* **265**(2), 112–118. doi: 10.1016/j.desal.2010.07.040

Langmuir, I. (1915) Chemical Reactions at Low Pressures. *J. Am. Chem. Soc.* **27**, 1139–1143.

Liu, C.H., Wu, J.S., Chiu, H.C., Suen, S.Y. & Chu, K.H. (2007) Removal of anionic reactive dyes from water using anion exchange membranes as adsorbers. *Water Res.* **41**, 1491–1500.

Madhavakrishnan, S., Manickavasagam, K., Vasanthakumar, R., Rasappan, K., Mohanraj, R. & Pattabhi, S. (2009) Adsorption of Crystal Violet Dye from Aqueous Solution Using Ricinus Communis Pericarp Carbon as an Adsorbent. *E-Journal of Chemistry* **6**, 1109–1116.

Miertschin, A. (2007) Kinetic *Study, Reaction of Crystal Violet with NaOH*. CHEM 213 Spring.

Mittal, A., Mittal, J., Malviya, A. & Gupta, V.K. (2010a) Removal and recovery of Chrysoidine Y from aqueous solutions by waste materials. *J. Colloid Interface Sci.* **344**(4), 497–507. doi: 10.1016/j.jcis.2010.01.007

Mittal, A., Mittal, J., Malviya, A., Kaur, D. & Gupta, V.K. (2010b) Adsorption of hazardous dye crystal violet from wastewater by waste materials. *J. Colloid Interface Sci.* **343**(4)**,** 463–473. doi: 10.1016/j.jcis.2009.11.060

Mohan, S. & Gandhimathi, R. (2009) Removal of Heavy Metal Ions from Municipal Solid Waste Leachate Using Coal Fly Ash as an Adsorbent. *J. Hazardous Mater.* **169**(2), 351-359. doi: 10.1016/j.jhazmat.2009.03.104

Monash, P. & Pugazhenthi, G. (2009) Adsorption of crystal violet dye from aqueous solution using mesoporous materials synthesized at room temperature. *Adsorption* **15**(3), 390–405.

Netpradith, S., Thiravetyan, P. & Towprayoon, S. (2004) Evaluation of metal hydroxide sludge for reactive dye adsorption in a fixed-bed column system. *Water Res.* **38**(10), 71–78.

Nidheesh, P.V., Gandhimathi, R., Ramesh, S.T. & Anantha Singh, T.S. (2011) Investigation of equilibrium and thermodynamic parameters of crystal violet adsorption onto bottom ash. *J. Intern. Environm. Appl. Sci.* **6**(4), 461–470.

Padmesh, T.V.N., Vijayaraghavan, K., Sekaran, G. & Velan, M. (2006) Biosorption of acid blue 15 using fresh water macroalga Azolla filiculoides, batch and column studies. *Dyes and Pigments* **71**(1), 77–82.

Rachakornkij, M., Ruangchuay, S. & Teachakulwiroj, S. (2004) Removal of Reactive Dyes from Aqueous Solution Using Bagasse Fly Ash. *Environm. Hazardous Manag.* **26**, 13–24.

Sarin, V., Singh, T.S. & Pant, K.K. (2006) Thermodynamic and breakthrough column studies for the selective sorption of chromium from industrial effluent on activated eucalyptus bark. *Biores. Technol.* **97**(16), 1986–1993. doi: 10.1016/j.biortech.2005.10.001

Selcuk, H. (2005) Decolorization and detoxification of textile wastewater by ozonation and coagulation processes. *Dyes Pigments* **64**(2), 217–222.

Sharma, D.C. & Foster, C.F. (1995) Column studies into the adsorption of chromium (VI) using sphagnum moss peat. *Bioresour Technol*. **52**(3), 261–267.

Song, J.Y., Zou, W.H., Bian, Y.Y., Su, F.Y. & Han, R.P. (2011) Adsorption characteristics of methylene blue by peanut husk in batch and column modes. *Desalination* **265**(3), 119–125. doi: 10.1016/j.desal.2010.07.041

Suksabye, P., Thiravetyan, P. & Nakbanpote, W. (2008) Column study of chromium (VI) adsorption from electroplating industry by coconut coir pith. *J. Hazardous Mater.* **160**(1), 56–62. doi: 10.1016/j.jhazmat.2008.02.083

Tan, I.A.W., Ahmad, A.L. & Hameed, B.H. (2008) Adsorption of basic dye using activated carbon prepared from oil palm shell, batch and fixed bed studies. *Desalination* **225**(1), 13–28. doi:

Weber JR, W.J. (1972) *Physico-chemical Process for Water Quality Control*. Wiley Inc, Newyork.

Zollinger, H. (2003) *Color Chemistry*. Wiley-VCH, Zurich, Switzerland.

Zulfadhly, Z., Mashitah, M.D. & Bhatia, S. (2001) Heavy metals removal in fixed-bed column by the macro fungus Pycnoporus sanguineus. *Environ Pollut.* **112**(5), 463–470. doi: 10.1016/S0269-7491(00)00136-6